

# A method for estimating apparent displacement vectors from time-lapse seismic images

Dave Hale, Colorado School of Mines

## SUMMARY

Reliable estimates of vertical, inline and crossline components of apparent displacements in time-lapse seismic images are difficult to obtain for two reasons. First, features in 3-D seismic images tend to be locally planar, and components of displacement within the planes of such features are poorly resolved. Second, searching directly for peaks in 3-D cross-correlations is less robust, more complicated, and computationally more costly than searching for peaks of 1-D cross-correlations.

We estimate all three components of displacement with a process designed to mitigate these two problems. We address the first problem by computing for each image sample a local phase-correlation instead of a local cross-correlation. We address the second problem with a cyclic sequence of searches for peaks of correlations computed for lags constrained to one of the three axes of our images.

## INTRODUCTION

Tiny displacements we observe in 3-D time-lapse seismic images are vectors, with three - vertical, inline, and crossline - components. These *apparent displacements* can be caused by reservoir compaction and are especially sensitive to related changes in strains and seismic wave velocities above reservoirs.

By “tiny”, we mean displacements that may be only a fraction of a sampling interval. Figures 1 show an example from time-lapse seismic imaging of a high-pressure high-temperature reservoir in the North Sea. Here we estimated vertical apparent displacements roughly equal to the time sampling interval of 4 ms. In the inline and crossline directions, we estimated horizontal apparent displacements of approximately 5 m, which is much less than the 25 m inline and crossline sampling intervals.

Though small, the most significant inline and crossline displacements appear to be correlated with the geometry of the target reservoir. The point of intersection of the three orthogonal slices in each of Figures 1 lies just beneath that reservoir.

Apparent vertical (time) displacements like those shown in Figure 1b tend to be downward (positive), even when physical reservoir boundaries are displaced upwards. This difference between physical and apparent vertical displacements has been observed and explained by Hatchell and Bourne (2005).

Apparent horizontal displacements are less well understood, although these too have been measured here and by others (e.g., Hall, 2006). Figures 1c and 1d show apparent displacements that are generally smaller in the inline direction than in the crossline direction.

Figure 1d implies that, near the reservoir, 3-D seismic images are pulling apart in the crossline direction as fluids are extracted. This apparent horizontal stretching is the opposite of the compaction that we might expect if we interpreted such displacements as physical movements of reservoir rocks. However, the apparent stretching we observe here is reasonable if we consider the effect of a mild low-velocity lens above the reservoir induced by compaction. If not accounted for in seismic migration (as it was not here), such a change in seismic velocity could explain these apparent crossline displacements.

Our understanding of apparent vector displacements today remains incomplete and beyond the scope of this paper. Our goal here is to describe the process by which we obtained these estimates of apparent

vector displacements from time-lapse seismic images.

Estimation of all three components of displacements is difficult. One difficulty is that displacements of image features are poorly resolved in directions parallel to those features. Therefore, in seismic images where features are often more or less horizontal, we tend to estimate only the vertical component of displacement, because only that component is well resolved.

A second difficulty is that some processing techniques used to estimate only a single vertical component of displacement do not extend easily to estimation of all three components. For example, estimating the locations of peaks of cross-correlations with sub-sample precision is straightforward when those correlations are functions of only vertical lag. A simple quadratic interpolation of correlation values near a sampled correlation peak may suffice. An extension of this processing to finding peaks in correlations that are a function of two or three components of lag is more complicated and less robust, partly because of the resolution problem described above.

Finally, estimation of three components of displacement requires more computation, and the increase in cost can be significant when estimating a complete field of displacement vectors for every sample in 3-D images.

This paper illustrates these difficulties and describes a process that mitigates them.

## LOCAL CROSS-CORRELATIONS

To facilitate visualization we consider only two components of displacement like those shown in Figures 2. The displacement vectors in this example correspond to compaction or squeezing of an image towards its center.

Using the displacement vector field shown in Figure 2, we can synthetically warp one seismic image to obtain another. The images in Figures 3a and 3b are related in this way. How might we recover the known displacement vectors from these two images?

One answer is to compute local cross-correlations. Hale (2006) describes an efficient method for computing a local multi-dimensional cross-correlation function for every image sample. Figures 3c and 3d show only a small subset of the normalized local cross-correlations computed for the upper-left quadrant of the images. These cross-correlations are made local by seamlessly overlapping Gaussian windows. They are normalized so that a correlation coefficient equal to one implies images that are locally identical except perhaps for constant relative shifts or amplitude scale factors.

The locations of peaks of local cross-correlation functions correspond directly to the components of displacement that we seek to estimate. Because displacements need not be integer multiples of sampling intervals, we must estimate these peak locations with sub-sample precision.

Figures 3c and 3d indicate a displacement of cross-correlation peaks vertically downward, which is consistent with the upper-left quadrant of Figure 2a. Horizontal (rightward) displacements of those peaks are more difficult to see. Displacements perpendicular to image features are more well resolved than those parallel to those features. In this example, estimates of vertical displacements shown in Figure 3e are more accurate than those of horizontal displacements shown in Figure 3f.

## Estimating apparent displacement vectors

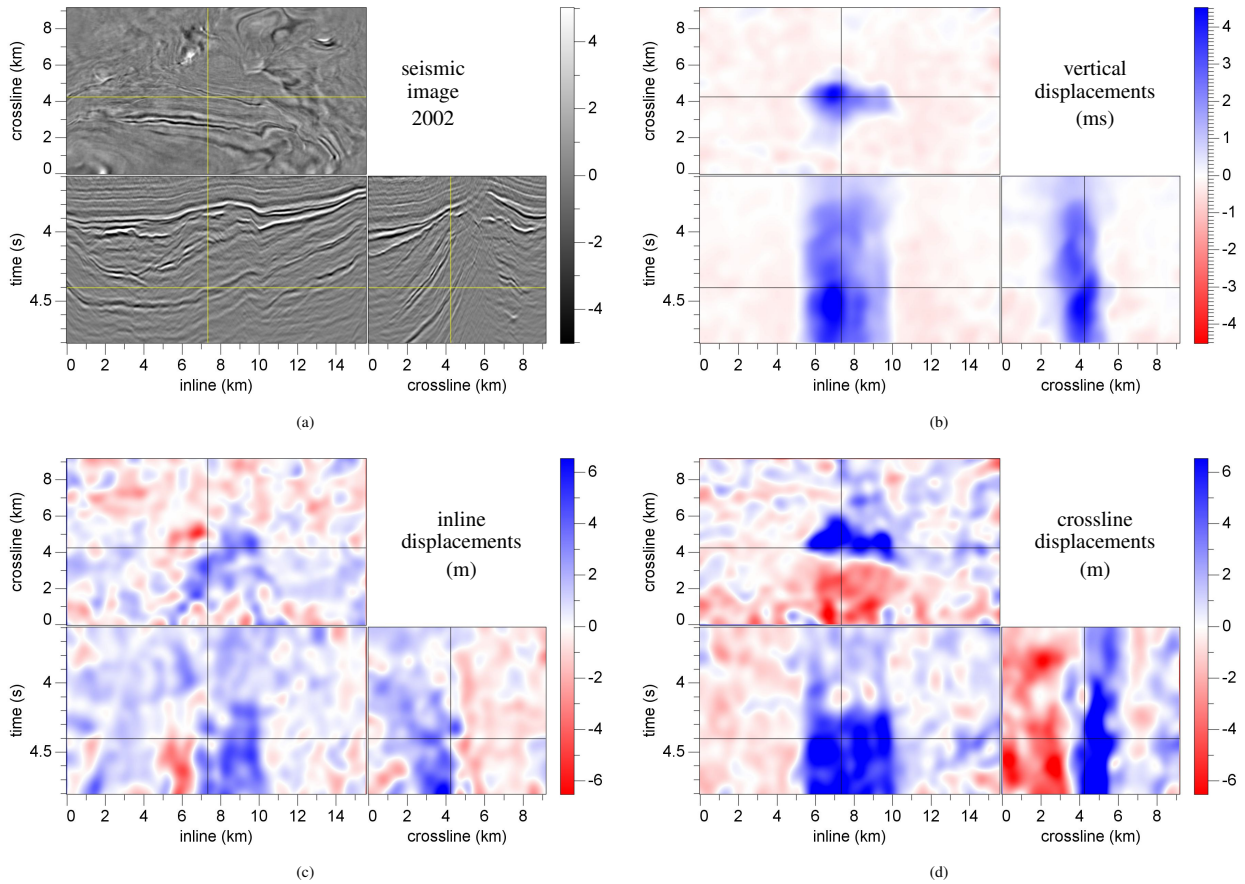


Figure 1: Slices (a) of a 3-D seismic image recorded in 2002. A second image (not shown) was recorded in 2004. Estimated vertical (b) components of apparent displacement are measured in ms; estimated inline (c) and crossline (d) components are measured in m. Crosshairs in each slice show the locations of the other two slices.

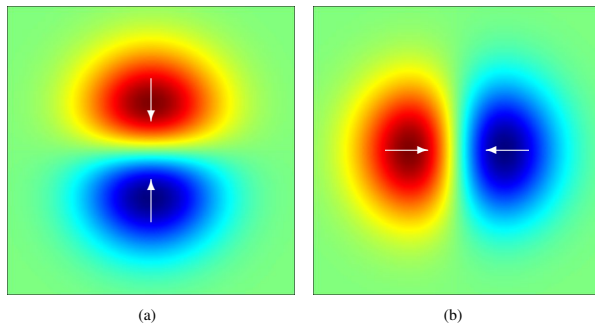


Figure 2: Vertical (a) and horizontal (b) components of a synthetic vector displacement field representing compaction of an image towards its center. Dark red denotes three samples of vertical displacement (a) downward or (b) toward the right. Dark blue denotes three samples of vertical displacement (a) upward or (b) toward the left.

### LOCAL PHASE-CORRELATIONS

The first step in our process is to improve the spatial resolution of cross-correlations in directions parallel to features in seismic images. We do this by applying spatially-varying multi-dimensional predic-

tion error filters to both images before cross-correlating them. These prediction error filters whiten the spectra of our images in all spatial dimensions.

Cross-correlation of whitened images is equivalent to phase-correlation, a process that is well known in the context of image registration (Kuglin and Hines, 1975). Phase-correlations are typically computed using Fourier transforms. Given two images that differ by only a constant shift, their Fourier transforms will differ only in their phase spectra. After spectral whitening, which amounts to simply dividing each Fourier transform by its amplitude spectrum, we can isolate this phase difference and recover the constant shift with sub-sample precision.

In our application Fourier transforms would be costly, because we compute a local cross-correlation and estimate a displacement vector for every image sample. To estimate a dense spatially varying vector field of apparent displacements, we instead approximate spectral whitening with local prediction error filters.

Prediction error filters have an undesirable side effect of amplifying high-frequency noise. Therefore, after local prediction error filtering we smooth the images with an isotropic Gaussian filter having half-width equal to one sample in all directions.

Figures 4 illustrate the effect that this processing step has on correlation functions and estimated apparent displacements. Phase-correlation peaks are well resolved in both vertical and horizontal directions. In Figures 4c and 4d we see horizontal displacements of those peaks that

## Estimating apparent displacement vectors

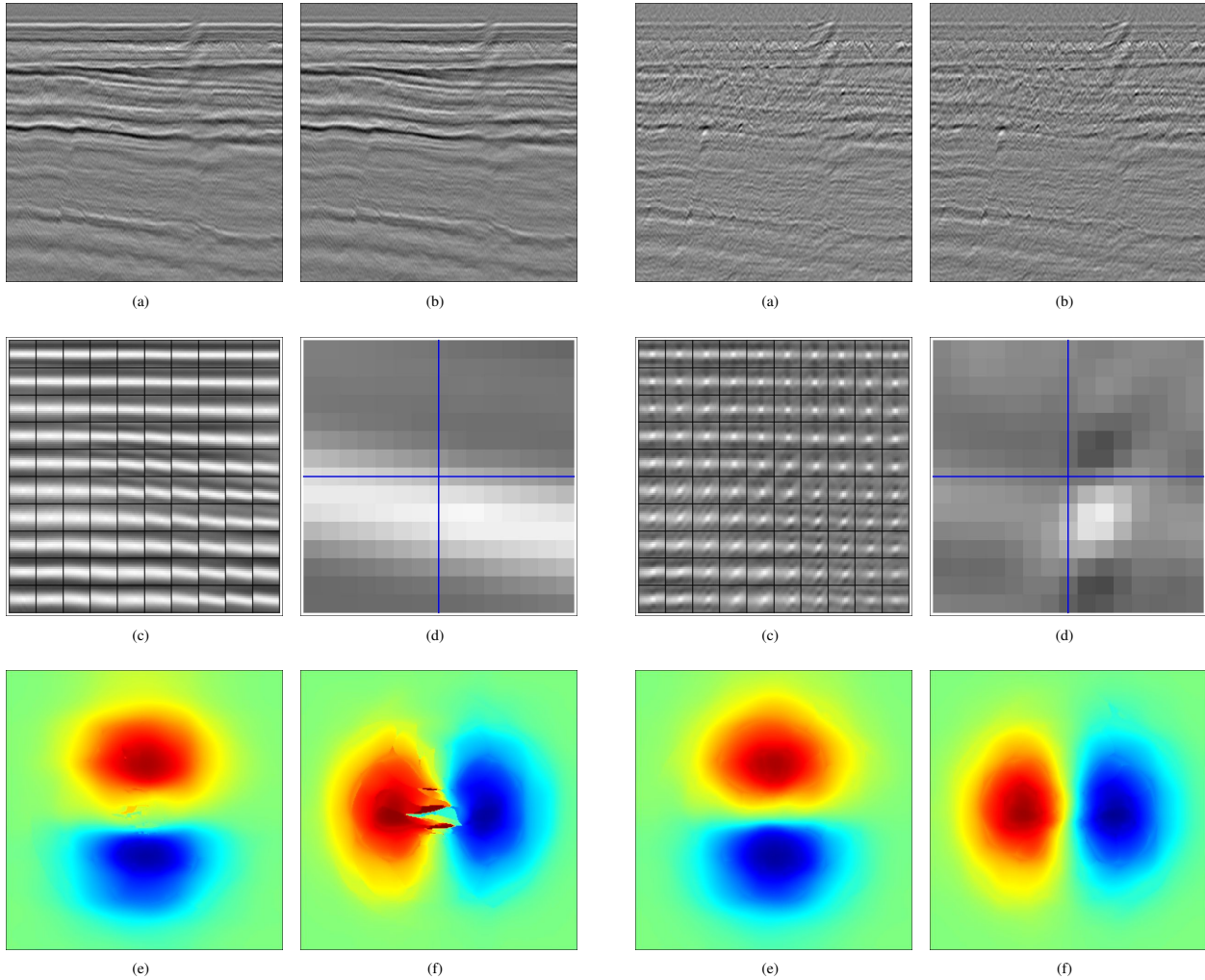


Figure 3: Estimates of displacement vectors from two  $315 \times 315$ -pixel images. The two images (a) and (b) are related by the displacements shown in Figure 2. The subset (c) of normalized local 2-D cross-correlations corresponds to the upper-left quadrant of these images, where displacements are downward and rightward. A downward shift is especially visible in one of these cross-correlations (d) shown in detail. A straightforward search for peaks of such cross-correlations yields estimates of both vertical (e) and horizontal (f) components of displacements.

are not apparent in Figures 3c and 3d. Because these peaks are more isotropic, estimated components of displacement in Figures 4e and 4f are more accurate than those in Figures 3e and 3f.

In the examples of Figures 3 and 4, we computed cross- and phase-correlation values for multiple integer lags and then least-squares-fit bi-quadratic functions to sampled correlation peaks. The components of displacement shown in these figures correspond to peaks of those quadratic functions. Unfortunately, quadratic functions in two and higher dimensions need not exactly interpolate any of the values nearest the sampled maximum correlation value.

For sampled correlations like those shown in Figures 3c and 3d, a least-squares-fit bi-quadratic may have a saddle point instead of a peak. In other words, in two dimensions, a peak may not exist for the quadratic fit to correlation values nearest to a sampled maximum value. And

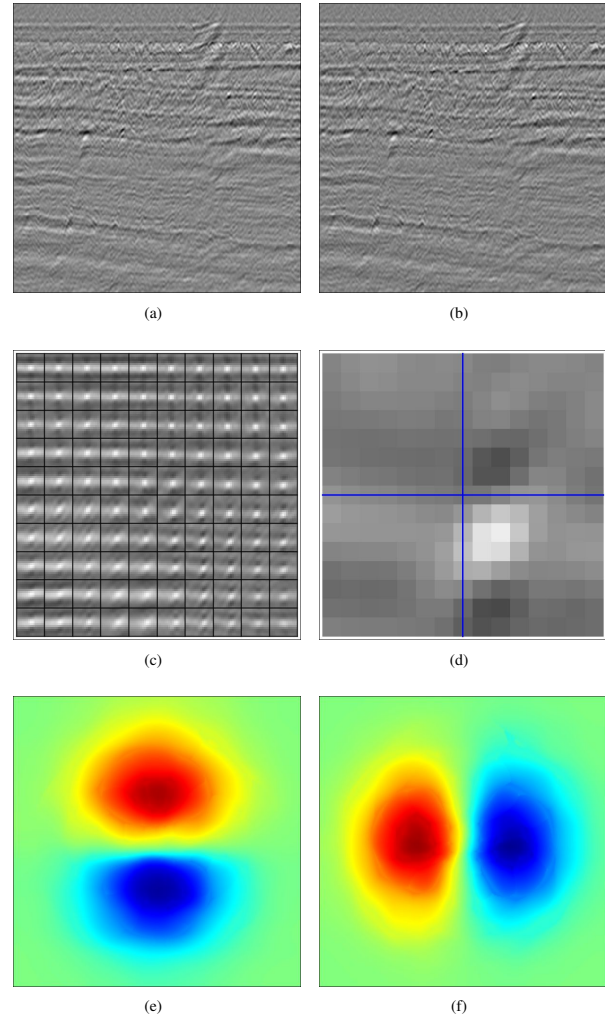


Figure 4: Images (a) and (b) after whitening with local prediction error filters and smoothing with an isotropic 2-D Gaussian filter. Smoothing attenuates high-frequency noise that is amplified by whitening, and facilitates location of the peaks of each of the phase-correlations shown in (c) and (d). Estimates of vertical and horizontal components of displacement in (e) and (f) are more accurate than those displayed in Figures 3e and 3f.

even when a quadratic peak does exist, it may be far away from the integer lag indices corresponding to the sampled maximum correlation value.

Such cases are pathological but not exceptional. We have observed them often while fitting bi-quadratic polynomials to the nine sampled values nearest the maximum sampled value in correlations like those shown in Figures 3c and 3d. Errors in quadratic fitting have been reduced but not eliminated in the example of Figures 4.

Another problem is the amount of memory needed to hold all of the correlation values required for fitting. For 2-D bi-quadratics, we must store 6 coefficients per image sample; for 3-D tri-quadratics, 10 coefficients per sample are required.

Fortunately, as described below, we can significantly reduce both the memory required and the number of correlation values computed, while eliminating errors due to quadratic fitting.

## Estimating apparent displacement vectors

### CYCLIC SEARCH

Following the whitening-and-smoothing step described above, the second step in our process is a cyclic sequence of correlations and shifts along each image axis.

We begin by cross-correlating two images in the vertical direction and finding the locations of peaks of those correlations. The Gaussian correlation windows remain multi-dimensional, but we restrict our computation of cross-correlation values to only vertical lags. The peak locations that we find for each image sample correspond to one component of the displacement vectors that we wish to estimate.

We then shift one of the images using high-fidelity sinc interpolation to compensate for our estimated vertical components of displacements. This interpolation aligns the two images by applying spatially varying vertical shifts to one of them.

After compensating for vertical displacements, alignment is incomplete where horizontal components of displacement are non-zero. We therefore correlate and shift horizontally to estimate and compensate for those horizontal components. After correlating and shifting for each image axis, we repeat the entire sequence of vertical and horizontal correlations and shifts until all shifts are negligible.

Figures 5 show estimated components of displacement for a four-cycle sequence of correlations and shifts. In each cycle we correlate and shift in both vertical and horizontal directions. Several features make this cyclic sequence of correlations and shifts attractive.

First, a cyclic sequence of one-dimensional searches for correlation peaks requires less memory than the direct multi-dimensional search used for Figures 3 and 4.

Second, in a cyclic search for correlation peaks we may compute fewer correlation values than in an exhaustive search over all possible 2-D or 3-D lags. In each correlate-and-shift step of cyclic search, we compute only one column or one row of cross-correlation values marked by the blue axes in Figure 4d.

Third, each quadratic interpolation we perform to locate peaks is guaranteed to find a peak value within one-half sample of the integer lag at which the maximum sampled correlation value occurs. No such guarantee exists for bi-quadratic and tri-quadratic fitting of 2-D and 3-D correlation values.

Finally, the cyclic sequence eliminates even small errors due to quadratic interpolation, because those errors go to zero as the shifts converge to zero. In each correlate-and-shift cycle, we compute shifts with quadratic interpolation, but we apply these shifts using a high-fidelity sinc interpolation. Therefore, errors in quadratic interpolation do not accumulate and are gradually eliminated.

The resulting estimates of displacement shown in Figures 5g and 5h are the most accurate of all such estimates shown in this paper. Compare these estimates with the known displacements in Figures 2.

In the 3-D example of Figures 1, we used two cycles of vertical-crossline-inline shifts. The shifts in the second cycle were large enough to be worth applying, but not so much as to warrant a third cycle.

### ACKNOWLEDGMENT

Thanks to Shell U.K. Limited and the Shearwater partnership (Shell, BP, and ExxonMobil) for providing access to their time-lapse seismic images and permission to publish results derived from them.

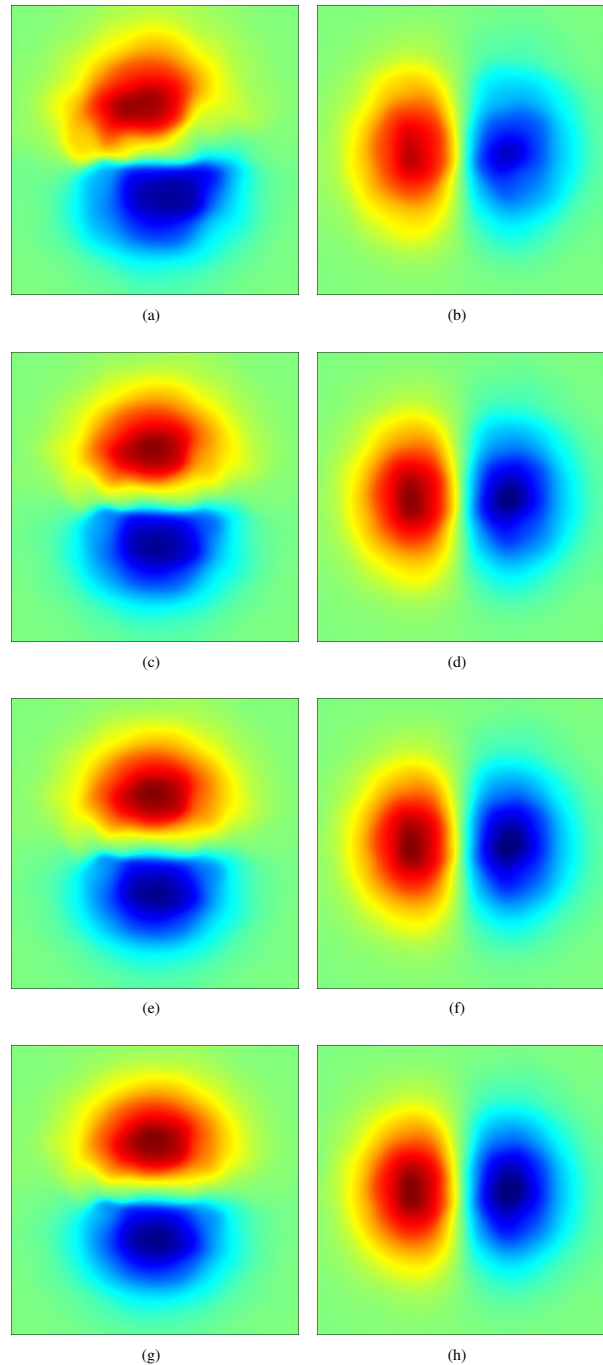


Figure 5: Four cycles of sequential estimation of two components of displacement for the images in Figures 4a and 4b. We first estimate vertical components of displacement (a). After shifting the image in Figure 4b vertically to compensate for these displacements, we estimate and compensate for horizontal components (b). Repeating this process, we obtain second (c and d), third (e and f) and fourth (g and h) estimates of displacements. Compare these final estimates with the known displacements in Figures 2.